Hydrogen Bond Formation between 4-(Dimethylamino)pyridine and Aliphatic Alcohols

Attila Demeter,* Viktória Mile, and Tibor Bérces

Institute of Materials and Environmental Chemistry, Chemical Research Center, Hungarian Academy of Sciences, 1025 Budapest, Pusztaszeri u. 59-67, Hungary

Received: April 17, 2007; In Final Form: June 4, 2007

The photophysics of 4-(dimethylamino)pyridine (DMAP) has been investigated in different solvents in the presence of aliphatic and fluorinated aliphatic alcohols, respectively. For most systems, consecutive two-step hydrogen-bonded complex formation is observed in the presence of alcohols. Equilibrium constants are determined from UV spectroscopic results for the formation of singly and doubly complexed species. The resolved absorption and fluorescence spectra for the singly and doubly complexed DMAP are derived by means of the equilibrium constants. Exceptionally large hydrogen bond basicity values are found for the ground and singlet excited DMAP molecules. In *n*-hexane, as a consequence of complex formation, the intramolecular charge transfer (ICT) emission becomes dominant over of the locally excited fluorescence; the fluorescence and triplet yields increase considerably with complexation. In polar solvents, both the fluorescence and triplet yields of the complex are much smaller than that of the uncomplexed DMAP. The dipole moments derived for the singly complexed species from the Lippert−Mataga analysis are much larger than those of the uncomplexed molecules. However, for the relaxed ICT excited-state one obtains different dipole moments in apolar and polar solvents. This may be explained by a conformational change of the molecule in the ICT excited state from planar geometry in apolar solvent to the perpendicular structure (characterized with bigger dipole moment) in polar solvent.

Introduction

Hydrogen bond formation of heterocyclic compounds with alcohols has been extensively studied in various solvents (see refs 1−4, and citations therein). Thus, for instance, in a previous study[5] we investigated the spectroscopy and thermodynamics of hydrogen bond formation of *N*-(2,6-dimethylphenyl)-2,3-naphthalymide (DMPN) with fluorinated alcohols in *n*-hexane. Complexation was found to occur both in the ground and in the excited singlet states. Beside other properties, the hydrogen bond basicity was determined for the hydrogen bond acceptor heterocyclic compound, as well as for the electronically excited molecule.

Relatively little is known on the hydrogen bond formation of dual luminescent compounds, and particularly how complex formation influences the spectroscopic and photophysical properties. In a recent study,[6] we obtained some information on the effect of hydrogen bond formation on the spectroscopy of the dual luminescent *N*-(2-fluorophenyl)- and *N*-(4-methoxyphenyl)-2,3-napthalimide derivatives. In accordance with expectation, it was found that hydrogen bond formation influences differently the short-wavelength and long-wavelength emitting excited-state properties.

A well-known and frequently studied[7−10] molecule is the 4-(dimethylamino)benzonitrile (DMABN), which belongs to a different type of dual luminescent compounds. Using transient IR spectroscopy, Phillips and co-workers[9] reported experimental evidence for formation of the hydrogen-bonded charge-transfer excited state of DMABN in methanol. This observation supports that hydrogen bond formation plays an important role in the photophysics of the donor−acceptor−substituted aromatics.

The smallest DMABN-like dual luminescent molecule is 4-(dimethylamino)pyridine (DMAP), which is the subject of the present study. The investigation of the photophysical properties of the 2-(dialkylamino)-5-cyanopyridine derivatives in methanol has contributed significant new experimental evidence[11] on the nature of the structural relaxation process of the ICT state of DMABN-like molecules.[7,8] The photophysics of the singlet excited DMAP species has been studied in different laboratories,[12−17] and the basic properties of the photophysics have been revealed. In polar solvents, the excited molecule shows dual luminescence with characteristics of the reversible two-state systems;[17] however, in apolar *n*-hexane, the long-wavelength fluorescence is almost unobservable. Due to their noncovalent bonding properties, the DMAP derivatives show some special features; for instance, they can be used in the stabilization of gold nanoparticles.[18]

In this paper, we study the effect of complexation of DMAP with different aliphatic alcohols (including fluorinated ones) in *n*-hexane solvent. In addition, systematic photophysical measurements were made and discussed for the DMAP−hexafluoro-2-propanol system in solvents of different polarity.

Experimental Methods

The absorption spectra were recorded on a thermoregulated Unicam UV500 spectrophotometer with a resolution typically of 0.5 nm. When necessary, correction was made for dilution caused by the addition of alcohol and for density change due to variation in temperature. The corrected fluorescence spectra were obtained on a Jobin-Yvon Fluoromax photon counting spectrofluorimeter with 0.5 nm resolution, as well as on a Perkin-Elmer LS 50B luminescence spectrometer. Excitation wavelength was around 285 nm. Room-temperature fluorescence quantum yields were determined relative to that of quinine

* To whom correspondence should be addressed. E-mail: demeter@chemres.hu.

10.1021/jp072989i CCC: $37.00
Published on Web 08/25/2007

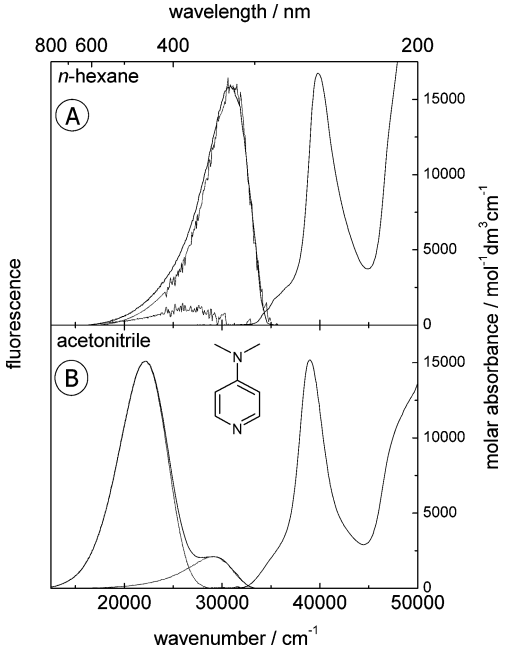

Figure 1. Absorption and fluorescence spectra of DMAP in *n*-hexane (A) and acetonitrile (B). (Dotted lines indicate the resolved LE and ICT emission.)

SCHEME 1

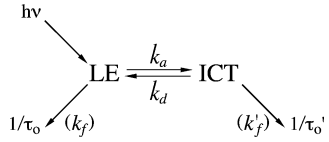

sulfate ($\Phi_f = 0.546$).[19] Time-resolved fluorescence measurements were made by the single-photon-counting technique.[5] In all measurements (except some absorption ones), deaereated samples were used. Absorption and fluorescence experiments were made at 25 °C, if not stated otherwise.

The triplet yields (Φ_{isc}) of DMAP and its complexed forms were measured at room temperature (23 ± 2 °C) by laser flash photolysis using the energy-transfer method with anthracene as energy acceptor.[20] The excitation wavelength was 266 nm, from a frequency-quadrupled Nd:YAG laser (Continuum Surelight). The measurements were made relative to the triplet yield either of *N*-methyl-1,8-naphthalimide in *n*-hexane ($\Phi_{isc} = 0.96$)[20] or of benzophenone in acetonitrile ($\Phi_{isc} = 1.00$).[20] In view of the relatively short triplet lifetime of the DMAPs (0.7−5 μs), a series of measurements were made with different concentrations of the quencher. The unbiased triplet yields were obtained by extrapolating the experimental data to infinite quencher concentration.

The DMAP**,** 4-(methylamino)pyridine (MAP), *N*,*N*-dimethylaniline (DMAN), and pyridine were obtained from Aldrich. The solid compounds were purified by crystallization from *n*-hexane, while the liquids by distillation followed by column chromatography on silica. Methanol (MeOH) was received from Fluka. The *n*-hexane for spectroscopy, ethanol (EtOH), and 2-propanol (IPA) were of Merck Uvasol quality and were used as received. Fluorinated alcohols (perfluoro-*tert*-butanol (PFTB), 1,1,1,3,3,3-hexafluoropropan-2-ol (HFIP**)**, 1*H*,1*H*,7*H*-dodecafluoroheptan-1-ol (DFH), 2,2,3,3,3-pentafluoropropan-1-ol (PFP), and 2,2,2-trifluoroethanol (TFE)) were purchased from Fluorochem Ltd. and were used without further purification.

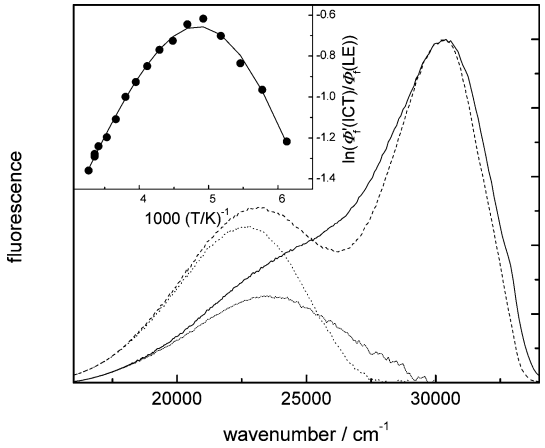

Figure 2. Fluorescence spectra of DMAP in diethyl ether at +25 (full line) and −70 °C (dashed line). The dotted lines indicate the contribution of the ICT emission to the total florescence. Inset: The Stevens−Ban plot of DMAP in DEE (see text).

Results and Discussion

(1) Absorption and Fluorescence Spectra of DMAP. The fluorescence spectrum of DMAP shows some mirror symmetry with the low-energy part of the absorption in *n*-hexane (Figure 1A), although the vibronic structure of the fluorescence spectrum is less developed. As seen from the long-wavelength region of the absorption spectrum, the lowest energy transitions are of forbidden character. In agreement with the literature,[16] density functional theory self-consistent field (DFT SCF) {6-311G++-(d,p)} Gaussian calculations indicate that the first three bands are characterized by low oscillator strengths and by moderate dipole moments. However, the fourth transition is of intramolecular charge-transfer character with high oscillator strength and considerable dipole moment pointing in the same direction as that in the ground state (i.e., the dimethylamino group has partial positive charge, while the aromatic ring carries negative charge). This transition can be assigned to the band with a maximum at 251 nm in the absorption spectrum (see Figure 1). Increasing the solvent polarity from *n*-hexane to acetonitrile, the low-energy region of the absorption spectrum is red-shifted by 5−6 nm (Figure 1B).

The character of the fluorescence spectrum changes considerably with the polarity of the solvent. At first view, in apolar *n*-hexane only the "locally excited" (LE, ^1L_b) emission is observable, the presence of a very weak "intramolecular charge transfer" (ICT, ^1L_a) emission becomes apparent only by comparison with the fluorescence spectrum of MAP in *n*-hexane. The mechanism and rate coefficients of the reversible two-excited-state system are shown in Scheme 1, where k_a and k_d are the rate constants of the forward and reverse reactions of ICT formation, τ_o (=$1/(k_{nr} + k_f)$) and $(k'_o)^{-1} = \tau'_o$ (=$1/(k'_{nr} + k'_f)$) are pseudolifetimes, whereas k_f(LE) and k'_f(ICT) are the radiative rate constants for the LE and ICT states, respectively.

In DEE, the ICT emission is well observable, although the LE emission is dominant (Figure 2). The ratio of the two fluorescence intensities changes considerably with decreasing temperature, while the overall fluorescence yield remains almost constant. The temperature dependence of the $\Phi_{f'}$(ICT)/Φ_f(LE) ratio, which is known as the Stevens−Ban plot,[21] is shown in the inset of Figure 2. Experimental data are fitted by the formula[9]

$$\ln\left(\frac{\Phi_f'(\mathrm{ICT})}{\Phi_f(\mathrm{LE})}\right) = -\frac{E_a}{RT} - \ln\left\{\left(\frac{k_f}{k_f'}\frac{A_d}{A_a}\right)\exp\left(\frac{(\Delta H^\circ - E_a)}{RT}\right) + \left(\frac{k_f}{k_f'}\frac{k_o'}{A_a}\right)\right\}$$

where the fitting parameters contain the A_a and A_d preexponential factors of the LE $\rightleftarrows$ ICT reaction. From the fitting, $E_a = 2.0 \pm 0.4$ kcal mol^{-1} and $\Delta H^\circ = -(1.5 \pm 0.2)$ kcal mol^{-1} are derived for the activation energy and reaction enthalpy of the reversible reaction shown in Scheme 1. Similar results ($E_a = 2.0$ kcal mol^{-1} and $\Delta H^\circ = -2$ kcal mol^{-1}) are given by Herbich and co-workers[17] from a Stevens−Ban plot measured for the same system in butyronitrile. In more polar solvents than DEE, well-developed dual luminescence has been detected (Figure 1B) in agreement with the results reported in the literature.[14,15,17]

The fluorescence quantum yield of DMAP**,** measured against quinine sulfate, is $\Phi_f = 0.002$ in *n*-hexane and increases considerably with increasing solvent polarity. The fluorescence decay is of multiexponential character. The dominant long component increases from 0.08 ns in *n*-hexane to 4.65 ns in polar butyronitrile ($\Phi_f = 0.015$).

The triplet yield is moderately low in *n*-hexane ($\Phi_{isc} = 0.18 \pm 0.02$), which is an indication for the presence of an effective internal conversion channel. This is often observed when two low-lying, vibrationally coupled excited states exist.[7] In agreement with the expectations, the triplet formation yield is considerably higher in acetonitrile ($\Phi_{isc} = 0.66 \pm 0.05$). The lifetime of the triplet excited molecule is short: 0.6 and 5.5 μs in *n*-hexane and acetonitrile, respectively. For the *N*,*N*-dimethylaniline, similarly short triplet decays were reported.[22]

(2) Absorption Properties of the Complexes. *(2.1) Influence of Alcoholic Additives on the Absorption Spectra in n-Hexane.* The effect of alcoholic additives on the DMAP absorption spectrum has been investigated in *n*-hexane using aliphatic alcohols and some fluorinated alcohols. The results obtained with HFIP are given in Figure 3. Addition of alcohol caused no considerable shift of the longer wavelength bands; it only increased the oscillator strengths. Such observations have been reported for partly forbidden transitions.[5,23] However, a very significant red shift is observed for the maximum of the absorption spectrum around 251 nm related to the ICT transition. The shift is explained as a consequence of the hydrogen-bonded complex formed in the interaction of DMAP with HFIP. An isobestic point is observed around 251.4 nm. An increase above 0.0033 mol dm^{-3} HFIP concentration results in the disappearance of the isobestic point, a decrease in the absorption band at 256.5 nm, and the appearance of a new absorption band at 275.0 nm. These observations can be explained by assuming a two-step consecutive complexation reaction mechanism. The absorption maxima at 250.8, 256.5, and 275.0 nm correspond to ICT transitions of the uncomplexed, singly complexed, and doubly complexed molecules, respectively.

On the basis of spectroscopic results, the complexation mechanism, given in Scheme 2, is suggested:

SCHEME 2

$$\mathrm{N} + \mathrm{X} \overset{K_1}{\rightleftharpoons} \mathrm{NX} \quad (1)$$

$$\mathrm{NX} + \mathrm{X} \overset{K_2}{\rightleftharpoons} \mathrm{NX_2} \quad (2)$$

where N is DMAP, X designates the complexing alcohol, and K_1 and K_2 are the equilibrium constants for the reversible formation of the singly and doubly complexed species, respectively. Assuming that dimerization of the alcohol is negligible; the expressions for the equilibrium concentrations of species N, NX, and NX_2 are given as[5]

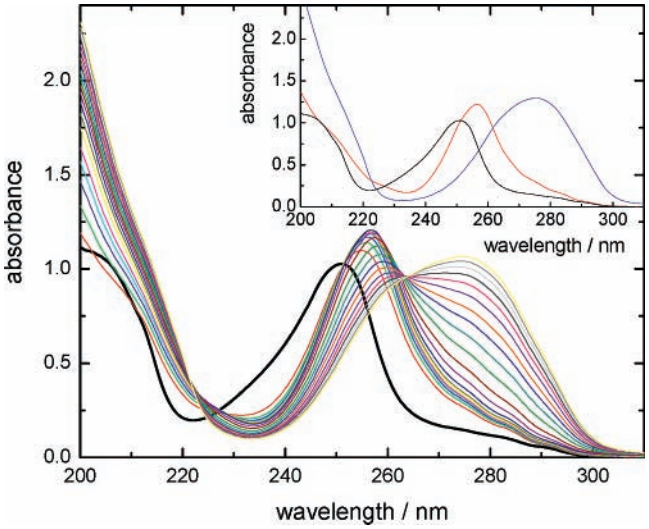

Figure 3. Absorption spectra of DMAP (6.14×10^{-5} mol dm^{-3}) with and without HFIP additive in *n*-hexane. (At 280 nm, the increasing absorbances correspond to 0, 0.00013, 0.00026, 0.00052, 0.0009, 0.0013, 0.0019, 0.0033, 0.0059, 0.011, 0.018, 0.028, 0.039, 0.050, 0.062, 0.076, 0.090, 0.105, 0.121, 0.137, and 0.154 mol dm^{-3} HFIP concentrations.) Inset: Resolved absorption spectra of the uncomplexed (black line), singly (red line), and doubly (blue line) complexed species.

$$[\mathrm{N}] = [\mathrm{N}]_0 - [\mathrm{NX}] - [\mathrm{NX_2}] \quad (3)$$

$$[\mathrm{NX}] = \frac{K_1[\mathrm{N}]_0[\mathrm{X}]}{1 + K_1[\mathrm{X}] + K_1K_2[\mathrm{X}]^2} \quad (4)$$

$$[\mathrm{NX_2}] = \frac{K_1K_2[\mathrm{N}]_0[\mathrm{X}]^2}{1 + K_1[\mathrm{X}] + K_1K_2[\mathrm{X}]^2} \quad (5)$$

The initial concentration of DMAP, $[N]_0$, can be determined easily from the absorbance of the sample which contains no alcohol. In the case of samples containing alcohol, the absorbance at a given wavelength may be calculated by the expression

$$A = \epsilon_N[\mathrm{N}] + \epsilon_{NX}[\mathrm{NX}] + \epsilon_{NX_2}[\mathrm{NX_2}] \quad (6)$$

where ϵ_N, ϵ_{NX}, and ϵ_{NX_2} are the molar absorption coefficients of species N, NX, and NX_2, respectively. In an iterative nonlinear fitting procedure, using Marquardt algorithm, K_1, K_2, and the molar absorption coefficients of complexes NX and NX_2 were optimized. In the fitting procedure, the absorbance measured at five selected characteristic wavelengths in samples with various alcohol concentrations was used.[5,6,23] In the case of the strongest hydrogen bonding alcohols, the consumption of the alcohol had to be taken into account.

The knowledge of the K_1 and K_2 equilibrium constants of complex formation allows us to derive the spectra for the singly complexed and doubly complexed species. Using the DMAP absorption spectrum, as well as the DMAP spectra measured in the presence of small alcohol concentrations (selected where the singly complexed species dominates) and relatively high alcohol concentration (selected where the contribution of the doubly complexed compound is most significant), the spectra of the singly and doubly complexed species are obtained by an iterative procedure (see for example the inset of Figure 3). The

maximum of the absorption band is shifted considerably to the red as a result of complex formation: the shift is 5.6 and 18.5 nm caused by the first and second complexation step, respectively. The molar absorption coefficients increase moderately by about 20% from DMAP to the DMAP−HFIP complex. The shape of the absorption spectrum of the doubly complexed species has a different character: the oscillator strength of the symmetry-forbidden low-energy transitions seems to increase considerably.

The complexation of DMAP was studied using also a number of alcohols other than HFIP. The alcohols included PFTB, DFH, PFP, TFE, methanol, ethanol, and 2-propanol. Equilibrium constants of complex formation and spectroscopic properties of the complexed species were determined. The main results are given in Table 1, where the complexing alcohols are listed in order of increasing hydrogen bond donating ability, characterized by the hydrogen bond acidity (α_2^H).[24] In this sequence, the equilibrium constants for the first as well as for the second complexation steps increase, indicating a decrease in the Gibbs energy change of complexation in the series. Thus it appears that the spectroscopic properties of the complexed species are significantly influenced by the Gibbs energy change in the complexation reaction.

(2.2) Hydrogen Bond Basicity of the Ground and Singlet Excited State of DMAP. Abraham et al.[24] expressed the logarithm of the equilibrium constant of hydrogen-bonded complex formation as a function of the product of the hydrogen bond acidity (α_2^H) of the donor and the hydrogen bond basicity (β_2^H) of the acceptor interacting species:

$$\log K = C_2 \alpha_2^H \beta_2^H - C_1 \qquad (7)$$

where the C_2 and C_1 parameters are reported to be $C_2 = 7.354$ and $C_1 = 1.094$ in carbon tetrachloride at 298 K. In Figure 4, the log K_1 value, measured for the DMAP−alcohol systems in *n*-hexane, is plotted against the α_2^H parameter of the alcohols. The intercept of the straight line is -2.2 ± 0.2, which is significantly lower than the -1.094 value reported by Abraham et al.[24] from numerous measurements made in carbon tetrachloride.

The experimentally determined slope of the plot is 8.53 ± 0.32, and the hydrogen bond basicity, derived from eq 7, is $\beta_2^H(\text{DMAP}) = 1.02 \pm 0.04$. Equation 7 was originally applied to measurements made in carbon tetrachloride. Later it was shown to be valid also in cyclohexane[25] and *n*-hexane,[5] but with slopes higher by about 14% (i.e., $C_2 = 8.384$). The β_2^H(DMAP) value is one of the biggest hydrogen bond basicity data ever published. (See some comparable values among phosphoric acid esters.)[24] This means that DMAP is an exceptionally good hydrogen bond acceptor.

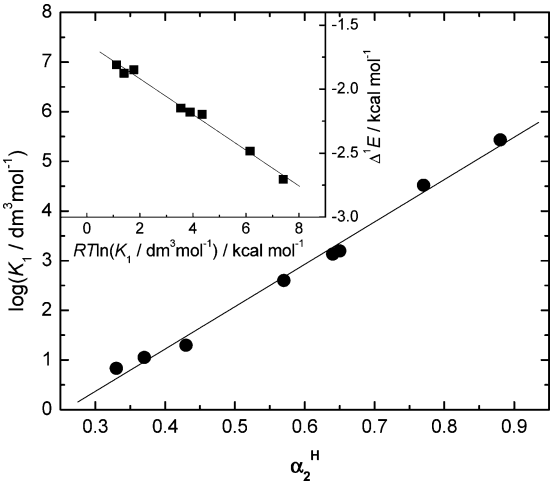

Figure 4. Logarithm of the equilibrium constant for complexation of DMAP as a function of hydrogen bond acidity of the alcohol in *n*-hexane. Inset: Singlet excitation energy difference of complexed and uncomplexed species (Δ^1E), derived from the absorption spectra, as a function of Gibbs energy change of complex formation ($-\Delta G° = RT \ln K_1$) in the DMAP−alcohol−*n*-hexane system at 25 °C. The sequence of alcohols from left to right is as follows: IPA, EtOH, MeOH, TFE, PFP, DFH, HFIP, and PFTB.

In Abraham et al.'s[24] empirical equation (eq 7), the C_1 parameter may be related to the entropy change in the complexation reaction. This seems to agree with the observation indicating that C_1 is more or less independent of the studied system. However, there are certain experimental results available which show that C_1 may differ from the usual value by as much as a factor of 2.[25] To investigate the question in more detail, $\Delta S°$ was derived experimentally from the van't Hoff plot for the DMAP−ethanol−*n*-hexane (between −10 and +60 °C) and DMAP−TFE−*n*-hexane (between 25 and 60 °C) systems. For both cases, $\Delta S_1°$ proved to be very similar (-23.6 ± 0.4 and -22.8 ± 0.9 cal mol^{-1} K^{-1}), while the reaction enthalpy — as expected — decreased with increasing hydrogen bond forming ability of the alcohol (-8.2 ± 0.1 kcal mol^{-1} for ethanol and -10.7 ± 0.5 kcal mol^{-1} for trifluoroethanol, respectively). The $\Delta S°$ values are much more negative than that which is determined for a typical case, such as for the pyridine−HFIP−*n*-hexane system ($\Delta S_1° = -10.8 \pm 2.9$ cal mol^{-1} K^{-1} and $\Delta H_1° = -7.0 \pm 0.9$ kcal mol^{-1}) or for the DMPN−HFIP−*n*-hexane system[5] ($\Delta S_1° = -12.4 \pm 1.8$ cal mol^{-1} K^{-1} and $\Delta H_1° = -6.5 \pm 0.1$ kcal mol^{-1}).

In a previous study,[5] dealing with complex formation between a 2,3-naphthalimide derivative and aliphatic alcohols, a linear relationship was found between the difference of the singlet excitation energy of the complexed and uncomplexed species on one hand and the room-temperature Gibbs energy change in the complexation reaction on the other hand:

TABLE 1: Spectroscopic and Equilibrium Parameters of Different DMAP−Alcohol Complexes in *n*-Hexane at 25 °C

alcohol	α_2^H	K_1 (dm^3 mol^{-1})	K_2 (dm^3 mol^{-1})	$\tilde{\nu}_{abs}^{max}$ (cm^{-1})	$\tilde{\nu}_f^{max}$ (ICT) (cm^{-1})	Φ_f
none				39 870	≈24 670	0.002
IPA	0.33[a]	6.8	0.5	39 234	24 370	0.006
EtOH	0.37[a]	10.9	1.7	39 210	24 100	0.014
MeOH	0.43[a]	19.8	1.9	39 220	24 500	0.006
TFE	0.57[a]	398	3.5	39 115	24 300	0.012
PFP	0.64[b]	720	5	39 104	24 550	0.013
DFH	0.65[a]	1 570	5	39 098	24 470	0.019
HFIP	0.77[a]	33 000	21	38 997	24 387	0.028
PFTB	0.88[b]	270 000	250	38 920	22 552	0.029

[a] Reference 24. [b] Reference 5.

$$\Delta^1E = {}^1E(\mathrm{NX}) - {}^1E(\mathrm{N}) = \frac{\beta_2^{\mathrm{H}}({}^1\mathrm{N}) - \beta_2^{\mathrm{H}}(\mathrm{N})}{\beta_2^{\mathrm{H}}(\mathrm{N})}\Delta G_1^\circ - RT\frac{\beta_2^{\mathrm{H}}({}^1\mathrm{N}) - \beta_2^{\mathrm{H}}(\mathrm{N})}{\beta_2^{\mathrm{H}}(\mathrm{N})}C_1' \quad (8)$$

where $C_1' = 2.303 \times 1.094$, which corresponds to the C_1 intercept in eq 7, and N and X designate the hydrogen donor and acceptor species, respectively. This relationship was explained by means of an energy cycle and Abraham's hydrogen bond acidity/basicity model.[5]

In the inset of Figure 4, the difference in the absorption maxima (Δ^1E) of the singly complexed and uncomplexed DMAP species are plotted as a function of the $RT \ln K_1$ at room temperature in *n*-hexane. The data indicate that a good linear correlation exists between Δ^1E and the Gibbs energy change in the complex formation reaction ($\Delta G^\circ = -RT \ln K_1$), just as is found in the case of the above-cited system. From eq 8, one can calculate the excited-state hydrogen bond basicity of the species in question $\{\beta_2^{\mathrm{H}}({}^1\mathrm{DMAP})\}$, if the corresponding ground-state value ($\beta_2^{\mathrm{H}}(\mathrm{DMAP}) = 1.02 \pm 0.04$) is known. Using this, $\beta_2^{\mathrm{H}}({}^1\mathrm{DMAP}) = 1.16 \pm 0.05$ can be derived from the slope (0.14 ± 0.01) of the inset of Figure 4. This value is bigger than the similarly large ground-state parameter. (The $\beta_2^{\mathrm{H}}({}^1\mathrm{DMAP})$ is derived from the absorption data; consequently it is an ICT excited-state property corresponding to the Frank−Condon ground-state configuration.)

(2.3) Location of Hydrogen Bonding in Singly and Doubly Complexed DMAP. To reveal where hydrogen bond formation occurs in the first and second complexation steps, the complexation of pyridine and *N*,*N*-dimethylaniline (DMAN), considered as models of the two functional groups in DMAP, were studied with alcohols in *n*-hexane. Cazeau and co-workers[12] stated that complexation with ethanol on the dimethylamino group is responsible for the formation of the ICT emission, while Herbich and Waluk[14] reported that complexation by butyl alcohol in *n*-hexane occurs on the pyridine nitrogen.

In the case of both pyridine and DMAN, the influence of HFIP additive on the spectra in *n*-hexane indicates a complexation mechanism consisting of two consecutive reversible reactions (see Figure 5). The equilibrium constants are relatively big for pyridine ($K_1 = 560$ dm^3 mol^{-1}, $K_2 = 11$ dm^3 mol^{-1}) and much lower for DMAN ($K_1 = 8.3$ dm^3 mol^{-1}, $K_2 = 3.7$ dm^3 mol^{-1}). In DMAP, the ICT character implies a relatively large negative charge on the pyridine moiety and a small electron density on the amino nitrogen. Thus, one expects bigger hydrogen bond accepting ability on the aromatic nitrogen atom for DMAP than for pyridine in accordance with the experimental results (note the much larger K_1 value of DMAP compared to that of pyridine). DFT calculations support this hypothesis. It turned out that the calculated energy change of the complexation reaction is much more negative if the alcoholic hydrogen of methanol interacts with the aromatic nitrogen ($\Delta E = -7.2$ kcal mol^{-1}) than if binding occurs at the amino nitrogen ($\Delta E = -2.8$ kcal mol^{-1}).

The binding location of the second interacting alcohol molecule raises an interesting problem: the second alcohol may attack (i) on the oxygen atom of the alcohol in the singly complexed species[26] (as it is probable in the case of complexation of pyridine and DMAN), (ii) on the nitrogen of the dimethylamino group, or (iii) on the π system of the aromatic ring. Spectral evidence suggests the second or the third possibility, since the UV spectrum of the doubly complexed species differs significantly from the singly complexed and uncomplexed species (see the inset of Figure 3). Note that if

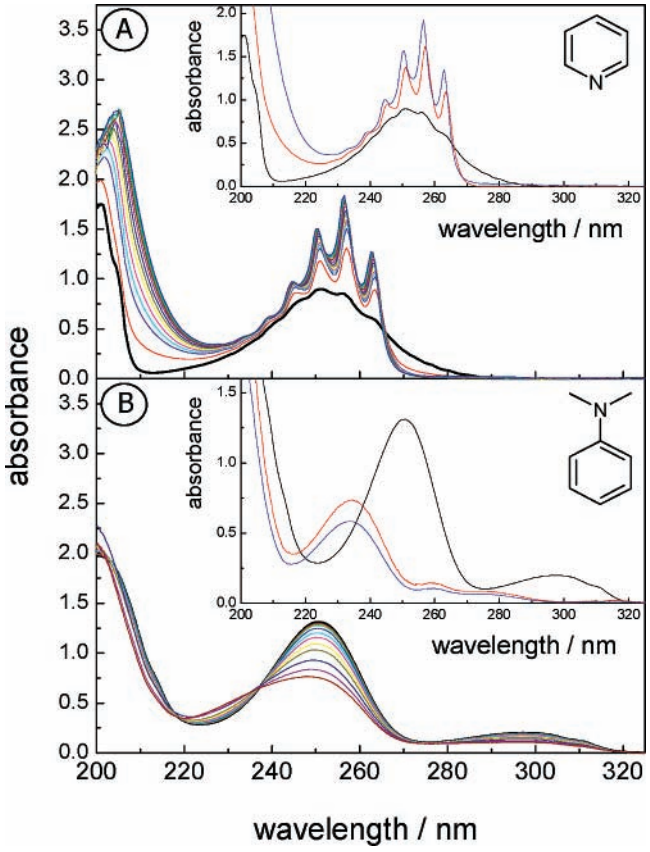

Figure 5. Absorption spectra of pyridine (4.3×10^{-4} mol dm^{-3}) (A) and *N*,*N*-dimethylaniline (8.1×10^{-5} mol dm^{-3}) (B) with and without HFIP additive in *n*-hexane. (The increasing absorbance corresponds to 0, 0.0034, 0.0069, 0.010, 0.017, 0.025, 0.036, 0.052, 0.069, 0.104, 0.175, 0.25, 0.36, and 0.54 mol dm^{-3} HFIP at 250 nm (A) and to 0, 0.0017, 0.0034, 0.0068, 0.012, 0.017, 0.026, 0.034, 0.051, 0.068, and 0.085 mol dm^{-3} HFIP at 230 nm (B).) Insets: Resolved absorption spectra of the uncomplexed (black line), singly (red line), and doubly (blue line) complexed species.

binding at the oxygen atom would dominate (case i), one would expect similar spectra for the doubly and singly complexed species with a small red shift of the former one.

(3) Fluorescence Properties of the Complexes. *(3.1) Fluorescence Spectra of Hydrogen-Bonded Complexes of DMAP in n-Hexane.* In contrast to the fluorescence spectrum observed for the uncomplexed DMAP in *n*-hexane, the singly complexed one shows well-developed dual luminescence. Moreover, the overall fluorescence yield increases by more than an order of magnitude as a result of complexation.

Derivation of the fluorescence spectrum of the singly complexed species was straightforward: due to the very low concentration of the alcohol applied (for example much less than 0.01 mol dm^{-3} HFIP in *n*-hexane), the excited-state processes could be neglected and the concentration ratio of the different species could be derived easily by means of the equilibrium constants and from the absorption properties of the ground-state system (see a detailed description in our earlier papers[5,23]). The fluorescence spectra of the species in question were derived at a minimum of three different alcohol concentrations in order to check the concentration independence. The emission spectrum of the DMAP−HFIP singly complexed species is shown in *n*-hexane in Figure 6A. The fluorescence quantum yield is 14 times bigger than that for the uncomplexed molecule in *n*-hexane. The long-time component of the ICT fluorescence decay increases considerably compared to the 0.08 ns value measured for the LE emission of the uncomplexed

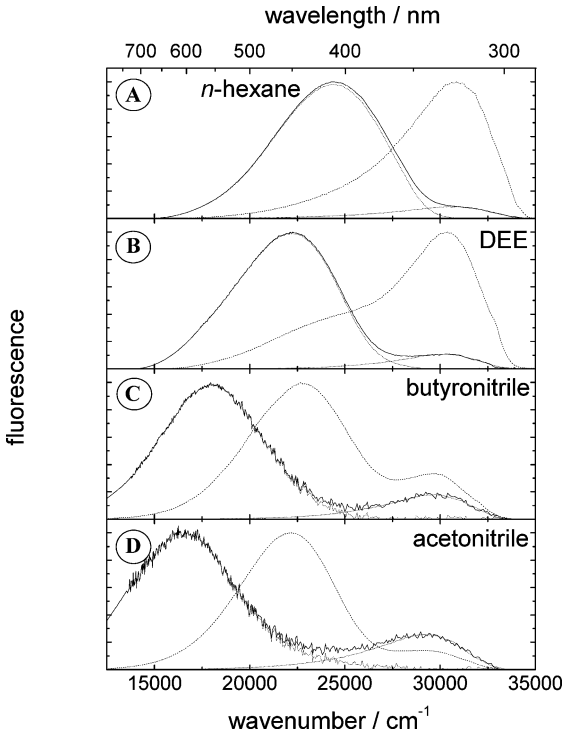

Figure 6. Fluorescence spectra of DMAP (dashed line) and the DMAP−HFIP complex (full line) in different solvents at room temperature. (Dotted line indicates the resolved LE and ICT emissions of the complex.)

molecule. (The corresponding value is 3.8 ns at 1.9×10^{-3} mol dm^{-3} HFIP concentration, where the 0.028 fluorescence quantum yield was determined. The decay parameter is slightly decreasing with increasing alcohol concentration.) The ICT fluorescence maximum is independent of the nature of most complexing alcohols; however, it shows a definite red shift for the strongest ones (see PFTB in Table 1). The triplet yield of the complexed species is significantly bigger than the uncomplexed one; for instance, it is $\Phi_{isc} = 0.76 \pm 0.5$ for the DMAP−HFIP complex. The triplet lifetime is not changed noticeably with complexation (it is around 0.8 μs). The fluorescence yield of the doubly complexed species is smaller by a factor of 5 than that of the singly complexed one; the yield is further decreasing with the increasing alcohol concentration. The ICT fluorescence maximum of the doubly complexed molecule is red-shifted by about 47 nm compared to the singly complexed species (which is around 21 900 cm^{-1} using HFIP additive in *n*-hexane).

(3.2) Fluorescence Spectra of the DMAP−HFIP Complexes in Polar Solvents. With increasing polarity of the solvent, the ICT emission of the uncomplexed DMAP becomes more and more visible, and in strongly polar solvents the ICT fluorescence is the dominant component of the emission. The singly complexed DMAP emits principally from the ICT singlet state in all solvents (Figure 6), while the fluorescence yield of the complexed species is decreasing with increasing polarity. The equilibrium constant K_1 decreases dramatically between *n*-hexane and the less polar ethers; however, thereafter it becomes practically independent of the solvent polarity (Table 2). The maximum of the ICT emission for the singly complexed molecule is strongly red-shifted compared to that observed for the uncomplexed one in polar solvents. The smaller fluorescence yield of the singly complexed molecule (when 0.05 mol dm^{-3} HFIP is added to butyronitrile) is in good agreement with the appearance of a new 0.5 ns component in the fluorescence decay of the ICT band. In accordance, the triplet yield decreases dramatically from 0.66 to 0.04 ± 0.03 as the result of complexation with a HFIP in acetonitrile.

(4) Solvatochromism of DMAP and Its Singly Complexed Derivative. Solvatochromic measurements were carried out to determine the LE and ICT state dipole moments of DMAP and its singly complexed derivative with HFIP. The energies corresponding to the maxima of the LE and ICT fluorescence bands can be described[27] by

$$\tilde{\nu}_f^{max} = \frac{-1}{4\pi\epsilon_0}\frac{2}{hc\rho^3}\mu_e(\mu_e - \mu_g^{FC})(f - f') + \text{constant} \quad (9)$$

In these equations, ρ is the equivalent spherical radius of the solute (Onsager radius) and ϵ_0 is the vacuum permittivity of the solvent, μ_e is the dipole moments either of the LE or the ICT states (μ_e(LE) and μ_e(ICT), respectively), whereas μ_g^{FC} represent the dipole moments of the Frank−Condon (FC) ground states reached upon emission from the LE or from the ICT states, μ_g^{FC}(LE) and μ_g^{FC}(ICT), respectively. (It is assumed here that μ_g^{FC}(LE) and μ_g^{FC}(ICT) are equal to the ground-state dipole moment μ_g of the relaxed molecules.) The solvent polarity parameter ($f - f'$) is defined by

$$f - f' = (\epsilon - 1)/(2\epsilon + 1) - (n^2 - 1)/(2n^2 + 1) \quad (10)$$

where ϵ and n are the dielectric constant and the refractive index of the solvent, respectively.

In Figure 7, the emission energies of the LE $\{\tilde{\nu}_f^{max}(LE)\}$ and ICT band $\{\tilde{\nu}_f^{max}(ICT)\}$ of DMAP and DMAP−HFIP are plotted against the solvent polarity function ($f - f'$).[27] To derive the dipole moments from the slopes of these plots by using eq 9, μ_g and ρ have to be known. For the μ_g value of DMAP**,** the experimentally determined[28] 4.22 D value was used, which is in reasonable agreement with the calculated values: 4.3,[14] 4.55,[16] and 4.83 D from this work. For the DMAP−HFIP complex, μ_g = 11 D was estimated from our DFT calculations, and this value was multiplied by the experimental/calculated ratio of DMAP to obtain 9.6 D for the dipole moment of the ground-state complex. The Onsager radii of DMAP and the DMAP−HFIP complex were derived relative to that of DMABN. The Onsager radius of DMABN was taken from the literature[27a] to be 4.20 Å, which corresponds to a 17 D dipole moment for the ICT excited state.[29,30] The ratio of molecular volumes of DMAP and DMABN**,** estimated by the atomic increment method of Edward,[31] is 259.7/310.2 = 0.837. With this ratio and the above-cited Onsager radius of DMABN**,** ρ = 3.96 Å is obtained for DMAP.

Szydlowska and co-workers[15] obtained the following lower values from DFT (B3LYP/6-311G(d,p)) calculations: their estimated ρ parameters are 3.3 and 3.8 Å for the planar and perpendicular conformers, respectively. According to this calculation the molecular volumes of the two conformers differ by about 50%; however, we find it more reasonable to use the same Onsager radius for both structures. For the ρ value of the DMAP−HFIP complex 4.8 Å is calculated using the Edward's method cited above.[31]

The solvatochromic shift of the absorption maximum belonging to the ICT transition can be analyzed by[27]

$$\tilde{\nu}_{abs}^{max} = \frac{-1}{2\pi\epsilon_0}\frac{2}{hc\rho^3}\mu_g(\mu_e^{FC} - \mu_g)(f - f') + \text{constant} \quad (11)$$

From the solvatochromic shifts of the absorption and fluorescence spectra of DMAP, summarized in Table 3 and

TABLE 2: Spectroscopic and Equilibrium Parameters of DMAP (N) and of the DMAP−HFIP Complex (NX) in Different Solvents at 25 °C

solvent	K_1 ($dm^3\ mol^{-1}$)	K_2 ($dm^3\ mol^{-1}$)	$\tilde{\nu}_{abs}^{max}$ (N) (cm^{-1})	$\tilde{\nu}_{abs}^{max}$ (NX) (cm^{-1})	$\tilde{\nu}_{f}^{max}$ (N) (cm^{-1})	$\tilde{\nu}_{f}^{max}$ (NX) (cm^{-1})	$-\Delta^1E$ (cm^{-1})	Φ_f(N)	Φ_f(NX)
n-hexane	33 000	21	39 832	38 997	24 670	24 387	837	0.002	0.028
dihexyl ether	160		39 637	38 800	24 115	23 400	720		
dibutyl ether	119		39 585	38 720	23 727	23 060	711	0.008	0.024
dipropyl ether	88		39 575	38 735	23 700	22 870	703		
diethyl ether	39		39 570	38 715	23 489	22 170	679	0.012	0.013
tetrahydropyrane	19.5		39 275	38 485	22 943	21 200	659		
ethyl acetate	33		39 220	38 505	23 048	20 405	674		
tetrahydrofurane	15		39 210	38 460	22 906	19 970	652	0.020	0.0031
methyl formiate	60.5	3.3	38 760	38 380	22 098	18 130	692		
valeronitrile	39.3	1.1	38 990	38 390	22 750	18 190	676		
butyronitrile	34.3	1.6	39 007	38 265	22 750	17 972	675	0.015	0.0009
propionitrile	25.4	1.1	38 945	38 270	22 358	17 209	667	0.017	0.0008
acetonitrile	23.1	5.8	38 965	38 150	22 114	16 567	664	0.012	0.0008

TABLE 3: Ground-State Dipole Moment, Onsager Radius, along with LE and ICT State Properties Related to Solvatochromic Measurements

	DMABN	DMAP	DMAP−HFIP
μ_g/D	6.6[a]	4.22[c]	9.6
ρ/Å	4.20[a]	3.96	4.8
slope (LE)/cm^{-1}	5700 ± 530[a]	5380 ± 400	4670 ± 420
slope (abs)/cm^{-1}	4800 ± 400	3180 ± 190	2970 ± 190
slope (ICT)/cm^{-1}	23 300 ± 2000[a,b]	7130 ± 700	14 420 ± 660[d]
			35 410 ± 1800[e]
μ_e(LE)/D	10.6[a]	8.2 ± 1.5	13.5
μ_e^{FC}(ICT)/D	12	8.9 ± 1.0	13
μ_e(ICT)/D	17[a]	9.2 ± 1.0	18.5[d]
			25.5[e]

[a] Reference 27a. [b] In ref 27a the 24 000 ± 2000 cm^{-1} value is derived using the reaction field of $f - 1/2f'$. [c] Reference 28. [d] Parameters derived in apolar solvents. [e] Parameters derived in more polar solvents than DEE.

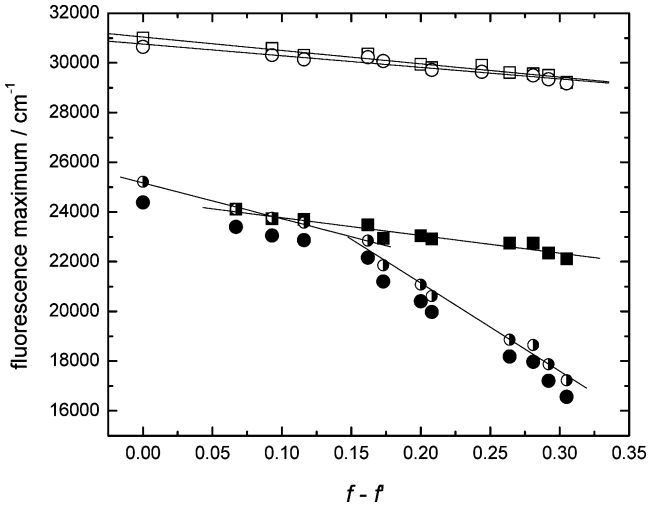

Figure 7. Plot of the wavenumber of the resolved emission maxima of the LE and ICT fluorescence (empty and full symbols, respectively) against the solvent polarity parameter $f - f'$. Data points: DMAP (□, ■); DMAP−HFIP (○, ●). The (◑) symbol indicates the corrected maximum of the ICT fluorescence of the complex (see text).

presented in Figure 7, the dipole moments of 8.9 and 9.2 D, respectively are derived for the ICT excited state. The smaller value corresponds to the ICT-state dipole moment at the geometry of the ground state (i.e., at the planar structure). This value is in excellent agreement with the 9.8 [14] and 8.6 [16] D results derived from semiempirical calculations.

The dipole moment of the relaxed ICT excited state was determined also by Herbich and co-workers[15] from the solvatochromic measurements of ICT fluorescence. Using only data measured in the most polar solvents, they found a bigger slope. When plotting their measurements according to eq 9, and applying lower Onsager radius than in the current work, a higher μ_e value was derived.

Our measurements show that the dipole moment of the ICT excited state changes only to a small extent due to relaxation (see Table 3). Using the same procedure to derive the dipole moments, different results are found with DMABN, where the dipole moment of the ICT excited state increases from 12 to 17 D as a result of relaxation. This is in excellent agreement with the DFT/MRCI calculations of Parussel,[30] where the value changes from 13.2 to 17.3 D. This observation may indicate that the structural relaxation plays a less important role in the formation of the ICT state in the case of DMAP.

The solvatochromic shift of the ICT absorption and the emission maxima of the DMAP−HFIP complex is definitively bigger than that of the uncomplexed DMAP. However, for a quantitative treatment one has to take into account the different singlet energy change of complex formation (Δ^1E) varying with the polarity of the solvent. The quantity Δ^1E can be calculated from eq 8 using the previously determined equilibrium constants (Table 2). Calculating by eq 11, from the absorption data a 13 D dipole moment is derived for the unrelaxed ICT state. From the fluorescence measurements made in apolar solvents (i.e., from *n*-hexane to diethyl ether), one may derive an 18.5 D dipole moment for the relaxed ICT excited state of the DMAP−HFIP complex. The fluorescence maxima determined in more polar solvents than that of the ethers (see Figure 7) imply a much bigger value: μ_e(ICT) = 25.5 D. All the dipole moments of the HFIP-complexed species are definitively larger than those of the uncomplexed DMAP (i.e., μ_g, μ_e(LE), μ_e^{FC}(ICT), and μ_e(ICT)). Hydrogen bonding on the heterocyclic nitrogen of DMAP markedly increases the dipole moment compared to that of the uncomplexed molecule both in the ground and the excited states (Table 3).

As an example, that the slope of the solvatochromic plot is much steeper in polar solvents than that found in weakly polar solvents, one may refer to the case of the fluorescence of quadrupolar chromophores.[32,33] The symmetry breaking of the electron distribution of the charge-transfer state in polar solvents results in larger solvent relaxation energy that the quadrupolar structure being otherwise more stable in an apolar environment. As a consequence, the shape of the corresponding Lippert−Mataga plot sharply deviates from linearity.

The value obtained in polar solvents is so high that it needs explanation. The different slopes of the Lippert−Mataga plot for less polar and more polar solvents than diethyl ether indicate a remarkable change. We consider two possible explanations:

(i) If an upper excited state exists with good hydrogen-bonding ability and very large dipole moment, this may lose enough energy by relaxation in polar solvents to become the lowest energy excited state (lower than the ICT state). Unfortunately, neither absorption spectroscopic nor theoretical evidence is available so far for the existence of such a state. (ii) A conformational change of the ICT excited state from planar geometry in apolar solvent (PICT)[8] to perpendicular structure in polar solvent (TICT)[7] could induce bigger dipole moment and as a consequence increase the red shift in the fluorescence spectrum. (Note that the quantum chemical calculations suggest that the dipole moment of the TICT state is larger than that of the PICT state in the case of DMABN.[30]) There are indications that the later explanation is more probable. An approximate estimate for the radiative rate constant of the ICT emission of the HFIP-complexed molecule may be done by simple division of the corresponding fluorescence yield and decay parameter, considering the exothermicity of the LE $\rightarrow$ ICT reaction. The k'_f(ICT) value decreases by more than a factor of 4, when one increases the solvent polarity from *n*-hexane to butyronitrile (i.e., from 7.4×10^6 to 1.8×10^6 s^{-1}), which effect does not contradict the suggested relaxation process (ii).

Fuss and co-workers[34] in their recent femtosecond study of DMABN discussed in detail the occurrence of the double minimum on the potential energy surface of the ^1L_a (ICT) state. Moreover semiempirical,[14] as well as DFT, calculations[16] for DMAP suggest that the ICT excited-state surface has a local energy minimum at the planar geometry (see Figure 4 of ref 14 and Figure 7 in ref 16). The possible change in conformation observed in the case of the DMAP−HFIP complex may occur for other systems (as, e.g., DMABN-related compounds) when energetically favorable conditions exist. It may be expected that in apolar solvents (as for instance paraffins) or crystalline environment[35] favor the planar geometry, while polar solvents would promote the formation of a more perpendicular structure.[7]

In the emission spectrum of DMAP in *n*-hexane, the ICT fluorescence is very weak; the Φ'_f(ICT)/Φ_f(LE) ratio is around 0.05. Similarly to DMABN,[8] the k'_f(ICT) value is lower than k_f(LE) by a factor of 8. This ratio is estimated from the fluorescence quantum yield and lifetime data measured in *n*-hexane and butyronitrile (see section 1), where the dominant emission comes from the LE and ICT states, respectively. Consequently, the LE $\rightleftarrows$ ICT reaction is endothermic by 0.5 kcal mol^{-1}, if the preexponential factors are equal or very similar (which is a reasonable assumption). The same endothermicity is obtained from the Stevens−Ban plot, derived from measurements in DEE (Figure 2), when the different energies in the two solvents are taken into account (see Figure 7).

As estimated from the location of the crossing point of the absorption and emission spectra (Figures 1, 3, and 6A), one can deduce that the singlet LE energy decreases from 96.5 to 96.2 kcal mol^{-1} due to HFIP complexation. From the difference of the absorption spectra, it is derived that the ICT-state energy decreases by 2.5 kcal mol^{-1}. Thus, we obtain that the LE $\rightleftarrows$ ICT reaction for the complex is exothermic by 1.7 kcal mol^{-1} in *n*-hexane compared with 0.5 kcal mol^{-1} endothermicity for the uncomplexed species.

Acknowledgment. This work was supported by the Hungarian Science Foundation (Grant OTKA T45890).

References and Notes

(1) Vinogradov, S. N.; Linnell, R. H. *Hydrogen Bonding*; Van Nostrand Reinhold: New York, 1971.

(2) Herbich, J.; Hung, C.-Y.; Thummel, R. P.; Waluk, J. *J. Am. Chem. Soc.* **1996**, *118*, 3508. Waluk, J. *Acc. Chem. Res.* 2003, *36*, 832.

(3) Dian, B. C.; Longarte, A.; Zwier, T. S. *J. Chem. Phys.* **2003**, *118*, 2696.

(4) Biczók, L.; Cser, A.; Nagy, K. *J. Photochem. Photobiol., A* **2001**, *146*, 59. Sebök-Nagy, K; Biczók, L. *Photochem. Photobiol. Sci.* **2004**, *3*, 390. Shimada, H.; Nakamura, A.; Yoshihara, T.; Tobita, S. *Photochem. Photobiol. Sci.* **2005**, *4*, 367. Miskolczy, Z.; Biczók, L.; Jablonkai, I. *Chem. Phys. Lett.* **2006**, *427*, 76. Krystkowiak, E.; Dobek, K.; Maciejewski, A. *J. Photochem. Photobiol., A* **2006**, *184*, 250. Coronilla, A. S.; Carmona, C.; Munoz, M. A.; Balon, M. *Chem. Phys.* **2006**, *327*, 70.

(5) Demeter, A.; Ravasz, L.; Bérces, T. *J. Phys. Chem. A* **2004**, *108*, 4357.

(6) Demeter, A. *React. Kinet. Catal. Lett.* **2005**, *85*, 331.

(7) Grabowski, Z. R.; Rotkiewicz, K.; Rettig, W. *Chem. Rev.* **2003**, *103*, 3899, and references therein.

(8) Druzhinin, S. I.; Ernsting, N. P.; Kovalenko, S. A.; Lustres, L. W.; Senyushkina, T. A.; Zachariasse, K. A. *J. Phys. Chem. A* **2006**, *110*, 2955. Zachariasse, K. A. *Chem. Phys. Lett.* **2000**, *320*, 8.

(9) Ma, C. S.; Kwok, W. M.; Matousek, P.; Parker, A. W.; Phillips, D.; Toner, W. T.; Towrie, M. *J. Phys. Chem. A* **2002**, *106*, 3294. Kwok, W. M.; George, M. W.; Grills, D. C.; Ma, C. S.; Matousek, P.; Parker, A. W.; Phillips, D.; Toner, W. T.; Towrie, M. *Angew. Chem., Int. Ed.* **2003**, *42*, 1826. Kwok, W. M.; Ma, C. S.; George, M. W.; Grills, D. C.; Matousek, P.; Parker, A. W.; Phillips, D.; Toner, W. T.; Towrie, M. *Phys. Chem. Chem. Phys.* **2003**, *5*, 1043.

(10) Dahl, K.; Biswas, R.; Ito, N.; Maroncelli, M. *J. Phys. Chem. B* **2005**, *109*, 1563.

(11) Dobkowski, J.; Wojcik, J.; Kozminski, W.; Kolos, R.; Waluk, J.; Michl, J. *J. Am. Chem. Soc.* **2002**, *124*, 2406. Dobkowski, J.; Michl, J.; Waluk, J. *Phys. Chem. Chem. Phys.* **2003**, *5*, 1027.

(12) Cazeau-Dubroca, C.; Nouchi, G.; Ben Brahim, M.; Pesquer, M.; Gorse, D.; Cazeau, Ph. *J. Photochem. Photobiol., A* **1994**, *80*, 125.

(13) Mishina, S.; Takayanagi, M.; Nakata, M.; Otsuki, J.; Araki, K. *J. Photochem. Photobiol., A* **2001**, *141*, 153.

(14) Herbich, J.; Waluk, J. *Chem. Phys.* **1994**, *188*, 247.

(15) Szydlowska, I.; Kyrychenko, A.; Nowacki, J.; Herbich, J. *Phys. Chem. Chem. Phys.* **2003**, *5*, 1032.

(16) Szydlowska, I.; Kyrychenko, A.; Gorski, A.; Waluk, J.; Herbich, J. *Photochem. Photobiol. Sci.* **2003**, *2*, 187.

(17) Szydlowska, I.; Kubicki, J.; Herbich, J. *Photochem. Photobiol. Sci.* **2005**, *4*, 106.

(18) Gandubert, V. J.; Lennox, R. B. *Langmuir* **2005**, *21*, 6532.

(19) Demas, J. N.; Crossby, G. A. *J. Phys. Chem.* **1971**, *75*, 991.

(20) Yoshihara, T.; Druzhinin, S. I.; Demeter, A.; Kocher, N.; Stalke, D.; Zachariasse, K. A. *J. Phys. Chem. A* **2005**, *109*, 1497. Suzuki, K.; Demeter, A.; Kühnle, W.; Tauer, E.; Zachariasse, K. A.; Tobita, S.; Shizuka, H. *Phys. Chem. Chem. Phys.* **2000**, *2*, 981, and references therein.

(21) Stevens, B.; Ban, M. I. *Trans. Faraday Soc.* **1964**, *60*, 1515.

(22) Tobita, S.; Kamiyama, R.; Takehira, K.; Yoshihara, T.; Yotoriyama, S.; Shizuka, H. *Anal. Sci.* **2001**, *17*, s50.

(23) Demeter, A.; Bérces, T. *J. Phys. Chem. A* **2005**, *109*, 2043.

(24) Abraham, M. H.; Duce, P. P.; Prior, D. V.; Barrat, D. B.; Morris, J. J.; Taylor, P. J. *J. Chem. Soc., Perkin Trans. 2* **1989**, 1355. Abraham, M. H. *Chem. Soc. Rev.* **1993**, *22*, 73.

(25) Abboud, J.-L. M.; Sraidi, K.; Abraham, M. H.; Taft, R. W. *J. Org. Chem.* **1990**, *55*, 2230.

(26) Frank, H. S.; Wen, W. Y. *Discuss. Faraday Soc.* **1957**, *24*, 133.

(27) Yoshihara, T.; Galievsky, V. A.; Druzhinin, S. I.; Saha, S.; Zachariasse, K. A. *Photochem. Photobiol. Sci.* **2003**, *2*, 342. Suppan, P.; Ghoneim, N. *Solvatochromism*; The Royal Society of Chemistry: Cambridge, U.K., 1997.

(28) Litonska, E.; Proba, Z.; Kulakowska, I.; Wierzchowski, K. L. *Acta Biochim. Pol.* **1979**, *26*, 39.

(29) Schuddeboom, W.; Jonker, S. A.; Warman, J. M.; Leinhos, U.; Kuhnle, W.; Zachariasse, K. A. *J. Phys. Chem.* **1992**, *96*, 10809.

(30) Parusel, A. B. J. *Phys. Chem. Chem. Phys.* **2000**, *2*, 5545.

(31) Edward, J. T. *J. Chem. Educ.* **1970**, *47*, 261.

(32) Amthor, S.; Lambert, C.; Dümmler, S.; Fischer, I.; Schelter, J. *J. Phys. Chem. A* **2006**, *110*, 5204.

(33) Terenziani, F.; Painelli, A.; Katan, C.; Charlot, M.; Blanchard-Desce, M. *J. Am. Chem. Soc.* **2006**, *128*, 15742.

(34) Fuss, W.; Schmid, W. E.; Pushpa, K. K.; Trushin, S. A.; Yatsuhashi, T. *Phys. Chem. Chem. Phys.* **2007**, *9*, 1151.

(35) Techert, S.; Zachariasse, K. A. *J. Am. Chem. Soc.* **2004**, *126*, 5593.